

SUPPORTING INFORMATION

Entropy-Driven Mechanisms in P2-Type Layered Oxide Cathodes for Sodium-Ion Batteries: New Insights from First-Principles and Electrochemical Analysis

Arianna Massaro,^{a,b,} Silvia Porporato,^{b,c} Miriam Botros,^{d,*} Alessandro Piovano,^{b,c,*} Hamideh Darjazi,^{b,c} David Stenzel,^d Giuseppina Meligrana,^{b,c} Ana B. Muñoz-García,^{b,e} Ben Breitung,^d Michele Pavone,^{a,b} and Claudio Gerbaldi^{b,c}*

^a Department of Chemical Sciences, University of Naples Federico II, Via Cintia 21, Napoli 80126, Italy

^b National Reference Centre for Electrochemical Energy Storage (GISEL), INSTM, Via Giusti 9, Firenze 50121, Italy

^c GAME Lab, Department of Applied Science and Technology (DISAT), Politecnico di Torino, Corso Duca degli Abruzzi 24, Torino 10129, Italy

^d Department of Physics “E.Pancini”, University of Naples Federico II, Via Cintia 21, Napoli 80126, Italy

^e Institute of Nanotechnology, Karlsruhe Institute of Technology (KIT), Hermann-von-Helmholtz Platz 1, 76344 Eggenstein- Leopoldshafen, Germany

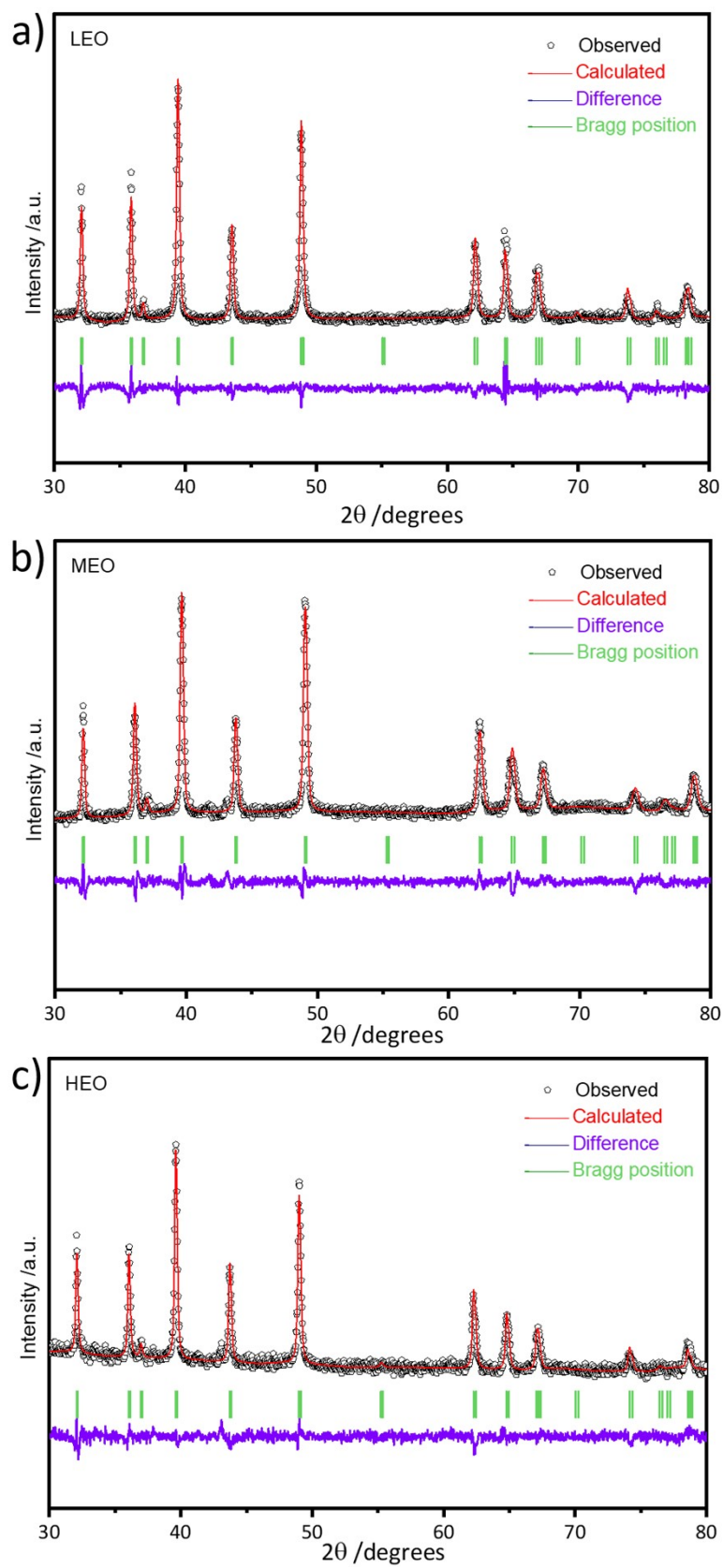


Figure S1. XRD patterns and Rietveld refinement results for (a) LEO (unweighted profile factor $R_p=2.6\%$), (b) MEO ($R_p=2.1\%$), and (c) HEO ($R_p=1.6\%$).

Table S1. Results of Rietveld refinement for the three samples, including lattice parameters (a , b , c), cell volume V , angles (α , β , γ), and unweighted profile factor R_p .

	a,b (Å)	c (Å)	V (Å³)	α, β	γ	R_p (%)
LEO	2.8912	11.1641	80.8198	90°	120°	2.6
MEO	2.8742	11.1385	79.6871	90°	120°	2.1
HEO	2.8757	11.1532	79.8741	90°	120°	1.6

Table S2. Lattice parameters of the minimum-energy structures for the $P2\text{-Na}_x\text{MO}_2$ series in their $8\times 4\times 1$ supercells as obtained at the PBE+U-D3BJ level of theory.

	LEO		MEO		HEO	
x_{Na}	a,b (Å)	c (Å)	a,b (Å)	c (Å)	a,b (Å)	c (Å)
0.68	23.272	11.233	23.097	11.155	23.127	11.169
0.50	23.165	11.181	23.007	11.112	22.808	11.487
0.30	23.097	11.149	23.031	11.123	22.773	11.469
0.12	22.951	11.078	22.927	11.073	22.794	11.480

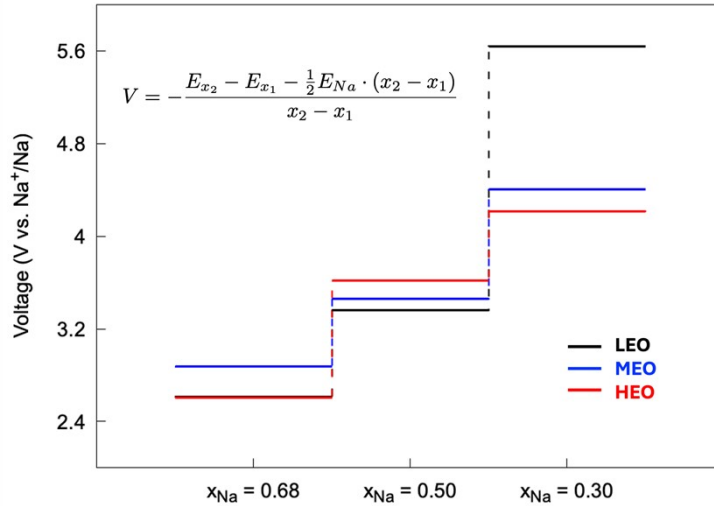


Figure S2. Capacity-voltage profile of $P2-Na_xMO_2$ compounds computed at PBE+U-D3BJ level of theory according to the displayed equation. Color legend is shown in the graph.

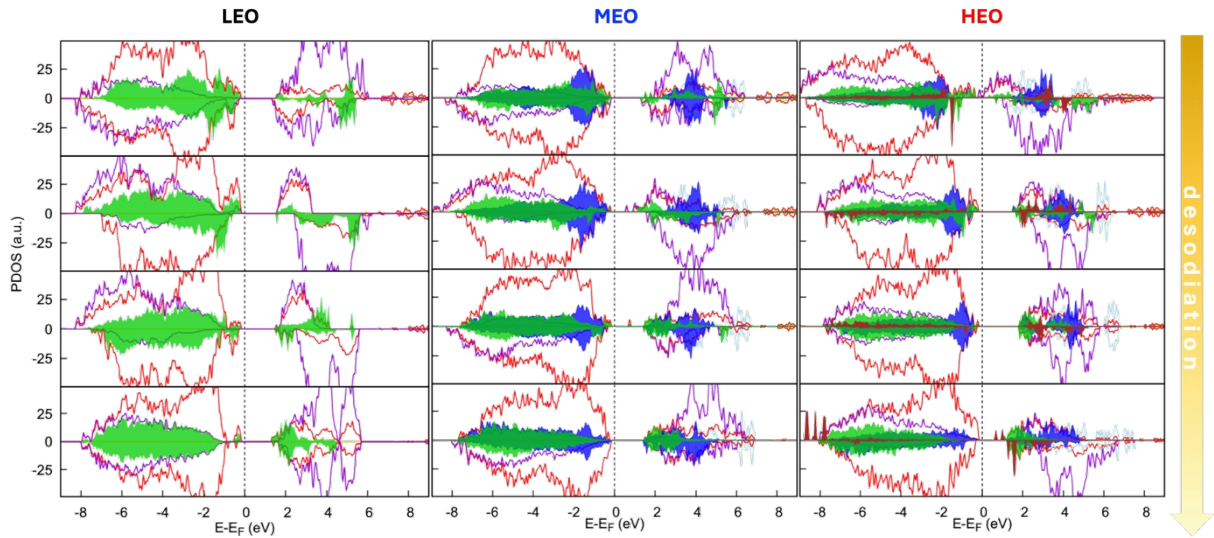


Figure S3. Atom- and angular momentum-projected density of states (PDOS) of LEO, MEO, and HEO as function of sodiation degree computed at HSE06 level of theory. Color code: Na s states, yellow; Mn d states, violet; Ni d states, green; Co d states, blue; Ti d states, cyan; Mg s states, orange; Al p states, grey; Fe d states, burgundy; O p states, red.

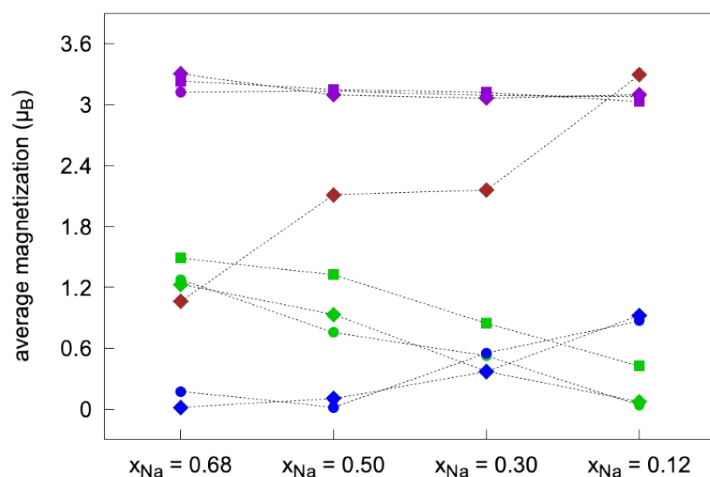


Figure S4. Average magnetization on Mn, Ni, Co and Fe sublattices in LEO, MEO and HEO as function of sodiation degree computed at HSE06 level of theory. Legend: Mn purple, Ni green, Co blue, Fe brown; LEO squares, MEO circles, HEO diamonds.

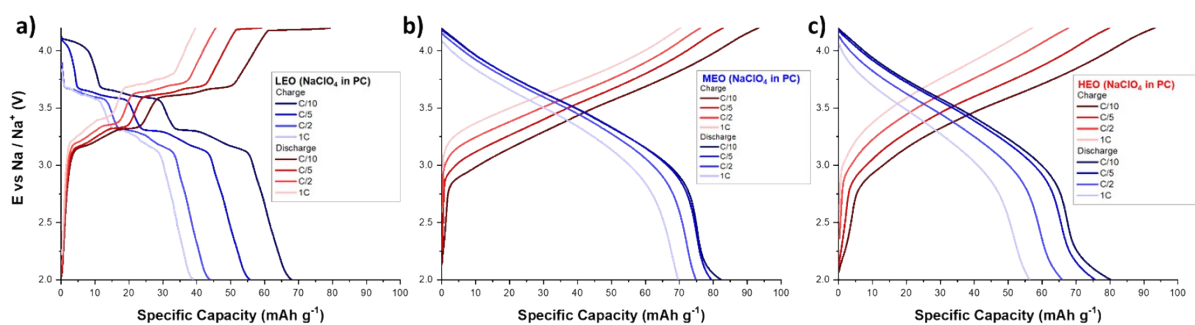


Figure S5. Representative voltage vs. specific capacity profiles recorded at different C-rates upon galvanostatic charge/discharge cycling of Na metal cells based on **a)** LEO, **b)** MEO, and **c)** HEO with standard electrolyte (NaClO_4 1M in PC), within the voltage range of 2.0–4.2 V vs Na^+/Na .

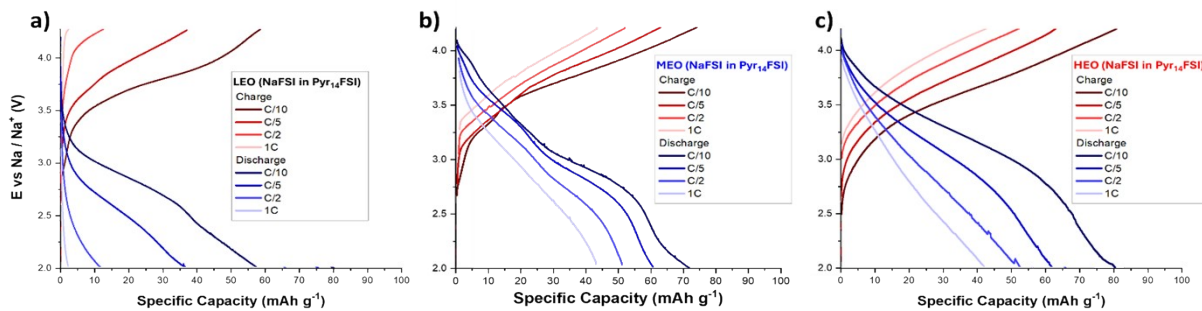


Figure S6. Representative voltage vs. specific capacity profiles recorded at different C-rates upon galvanostatic charge/discharge cycling of Na metal cells based on **a)** LEO, **b)** MEO, and **c)** HEO with standard electrolyte (NaFSI in Pyr₁₄FSI 1:4), within the voltage range of 2.0–4.2 V vs Na⁺/Na.

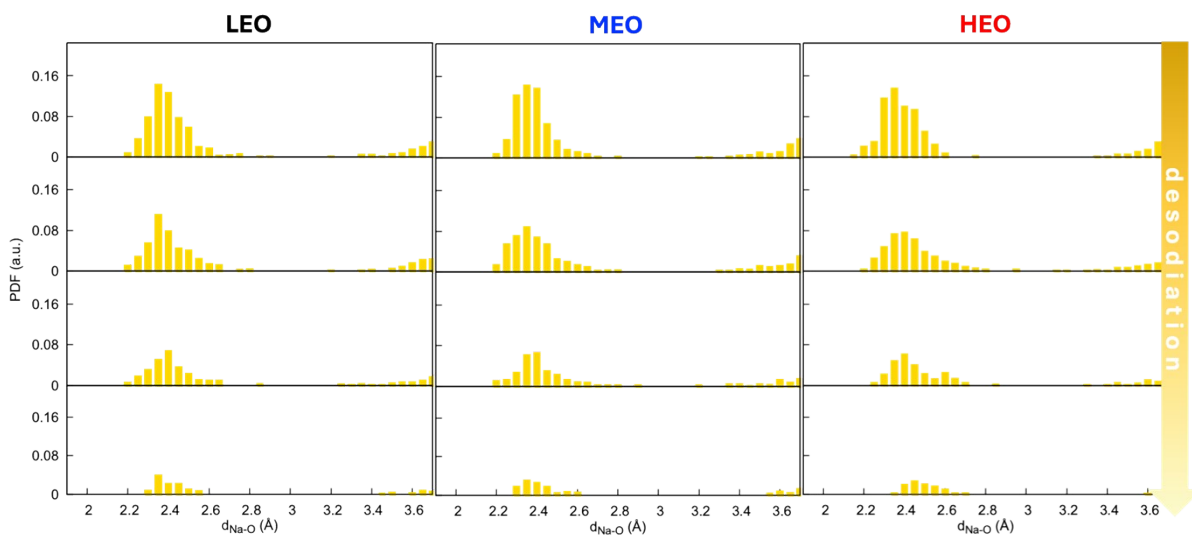
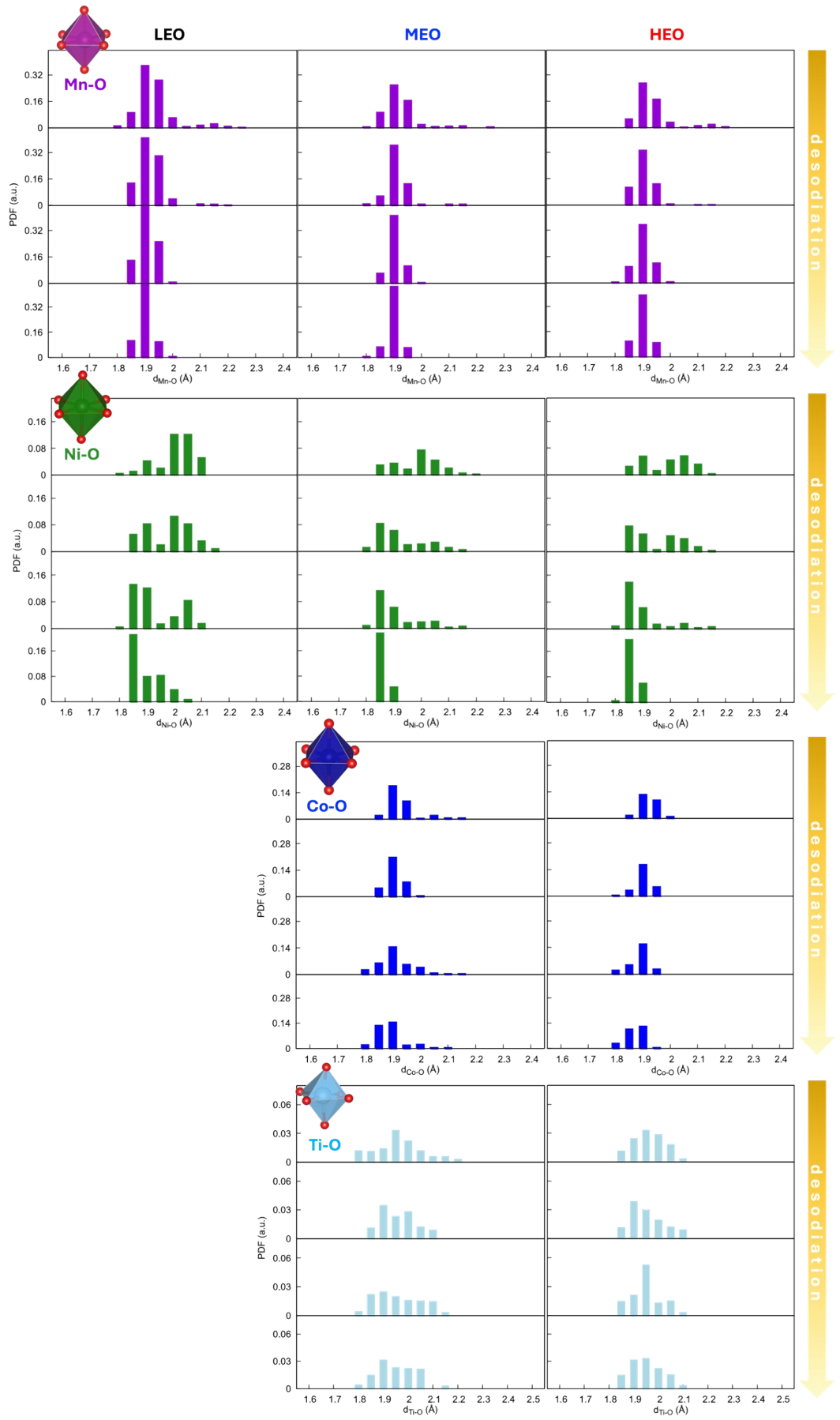


Figure S7. Pair distribution function of Na-O distances computed for the PBE+U-D3BJ minimum-energy structures of LEO, MEO and HEO at different sodiation stages.



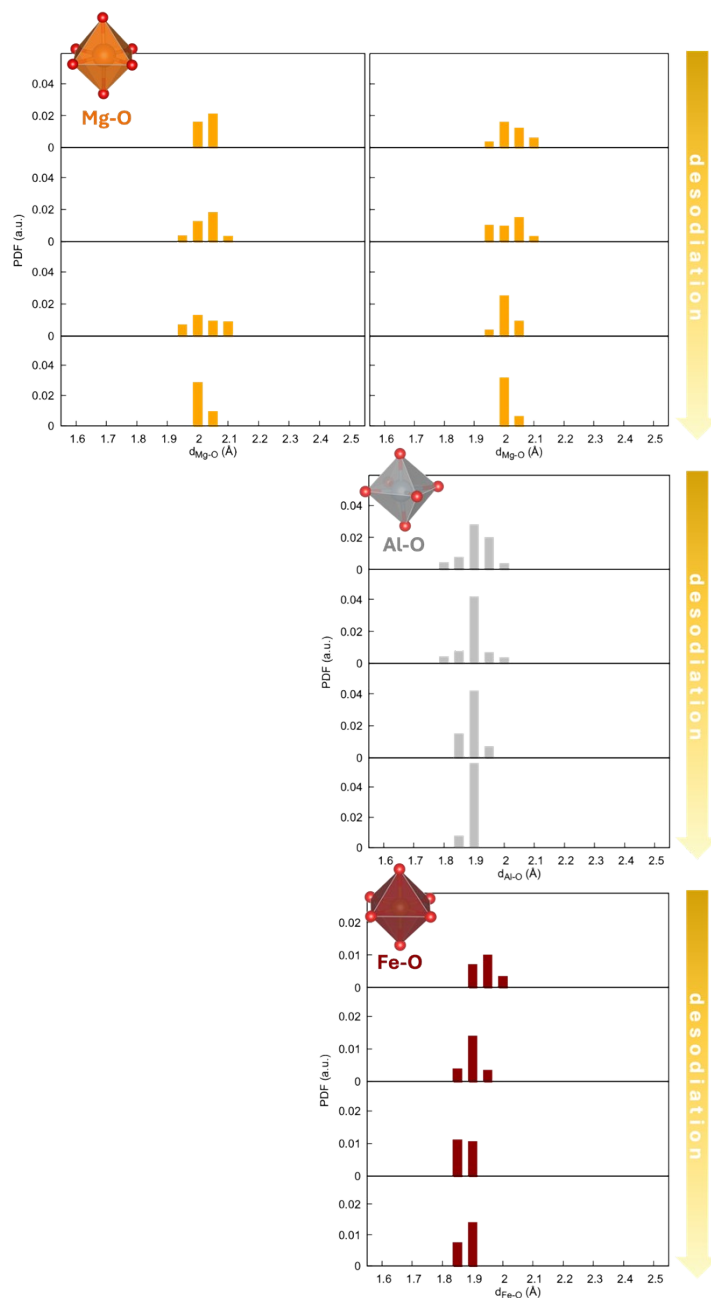


Figure S8. Pair distribution function of M-O distances computed for the PBE+U-D3BJ minimum-energy structures of LEO, MEO and HEO at different sodiation stages.